

Spin Dependent Hopping and Colossal Negative Magnetoresistance in Epitaxial $\text{Nd}_{0.52}\text{Sr}_{0.48}\text{MnO}_3$ Films in Fields up to 50 T

P. Wagner,* I. Gordon, L. Trappeniers, J. Vanacken, F. Herlach, V. V. Moshchalkov, and Y. Bruynseraede

Laboratorium voor Vaste-Stoffysica en Magnetisme, Katholieke Universiteit Leuven, Celestijnenlaan 200 D, 3001 Leuven, Belgium

(Received 7 April 1998; revised manuscript received 19 August 1998)

The low carrier mobility of the magnetic perovskite $\text{Nd}_{0.52}\text{Sr}_{0.48}\text{MnO}_3$ implies that the dominant conductivity mechanism is related to Mott hopping. We propose a modification of Mott's original model by taking into account that the hopping barrier depends on the misorientation between the spins of electrons at an initial and a final state in an elementary hopping process. Using this model we deduce a negative-magnetoresistivity scaling proportional to the Brillouin function \mathcal{B} in the ferromagnetic state and to \mathcal{B}^2 in the paramagnetic state. Both predictions are in full agreement with the magnetoresistivity measured in pulsed magnetic fields up to 50 T. [S0031-9007(98)07410-9]

PACS numbers: 75.70.Pa, 73.50.Jt, 75.70.Ak

Rare earth (RE) manganites REMnO_3 with divalent substitution on the RE site show a transition from a paramagnetic-semiconducting to a ferromagnetic-quasimetallic state at the Curie temperature T_C . Many of these compounds exhibit also colossal negative magnetoresistivity (CMR) [1,2], being most pronounced in the vicinity of T_C . Additional phenomena like charge and orbital ordering occur for special substitution ratios (e.g., 25% or 50% divalent ions), resulting in interrelated structural, magnetic, and electric phase transitions [3,4]. The electric conduction in the RE manganites is usually ascribed to polaron hopping in the paramagnetic state [5], and to the double-exchange (DE) mechanism for the ferromagnet [6], with the charge transfer integral depending on the relative spin orientation of neighboring Mn^{3+} and Mn^{4+} sites. It was recently shown that DE alone is insufficient to explain all magnetotransport properties and that the coupling of carriers to the lattice and its distortions must be taken into account [7]. The importance of these lattice deformations (Jahn-Teller polarons) was illustrated by the oxygen-isotope effect found in $\text{La}_{0.8}\text{Ca}_{0.2}\text{MnO}_3$ [8]. The original DE model and related theories have in common, however, that CMR is caused by a magnetic field-induced enhancement of the carrier mobility while the carrier density is not affected. This basic assumption has been confirmed for the ferromagnetic state by Hall-effect studies on $\text{Nd}_{0.5}\text{Sr}_{0.5}\text{MnO}_3$ thin films [9].

A central question is the temperature and magnetic field dependence of the resistivity and the magnetization. Several authors reported on the *phenomenological observation* that the resistivity decrease as a function of field is related to the magnetization M for the ferromagnet and to M^2 for the paramagnet [10]. Since the main difference between both phases is the existence of a spontaneous magnetization, it is tempting to deduce the two, apparently different CMR scaling laws from a more universal approach. This would also imply that there is possibly no intrinsic difference between the quasimetallic transport mechanism below T_C and the semiconducting mechanism above T_C . Although this approach does not need to hold globally for

all CMR materials, it seems promising at least for the less conducting compounds. These materials exhibit similar resistivities in the ferromagnetic and in the paramagnetic state, and the field-induced resistance drop does not result in metalliclike conductivity values.

In this Letter we will discuss the magnetoresistivity of a RE manganite with roughly 50% divalent substitution ($\text{Nd}_{0.52}\text{Sr}_{0.48}\text{MnO}_3$) within both magnetic phases. Pulsed magnetic fields up to 50 T allow to induce even in the paramagnetic state an almost parallel alignment of magnetic moments, and we show that the resulting conductivity achieves values typical for the ferromagnet. The different CMR scaling in both magnetic phases will be deduced from a hopping model, taking into account the influence of temperature (Weiss field) and external magnetic fields on the spin-misorientation contribution into the effective hopping barrier.

The $\text{Nd}_{0.52}\text{Sr}_{0.48}\text{MnO}_3$ thin films were prepared *in situ* by dc-magnetron sputtering onto (100) SrTiO_3 substrates [11]. The epitaxial growth was confirmed by x-ray diffraction, and the composition analysis by Rutherford backscattering gave a Nd/Sr ratio of 0.52/0.48. The magnetic properties were investigated with a SQUID magnetometer, allowing to determine the Curie temperature $T_C = 207$ K. For transport measurements in pulsed magnetic fields [12] we used a 10×2.8 mm² sample (film thickness 3000 Å) with four evaporated and annealed gold electrodes. The field axis was within the sample plane and parallel with the measuring current. The temperature dependence of resistivity at different fields is shown in Fig. 1. At the lower fields a transition from a semiconductorlike behavior in the paramagnetic phase to a quasimetallic behavior in the ferromagnetic regime is clearly visible. Increasing external fields causes a shift of this transition to higher temperatures. Charge ordering does not occur, probably due to the small deviation from the ideal Nd/Sr ratio of 0.50/0.50 [4].

We performed magnetoresistance measurements up to 50 T in the paramagnetic phase, near T_C , and in the ferromagnetic phase down to 10 K. Before applying the field

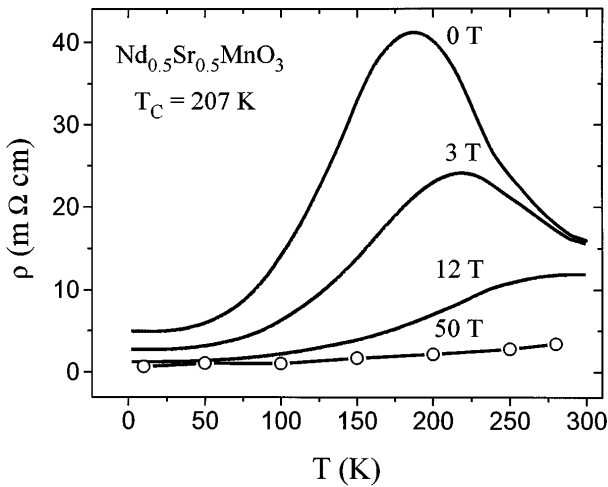


FIG. 1. Temperature-dependent resistivity of an epitaxial $\text{Nd}_{0.52}\text{Sr}_{0.48}\text{MnO}_3$ film in zero external field and in fields of 3, 12, and 50 T, respectively. Open dots refer to pulsed-field measurements.

pulse the sample was thermally cycled to room temperature and zero field cooled to the nominal measurement temperature. The temperature changed less than ± 0.5 K during the pulse duration of ≈ 20 ms. The field-induced resistivity decrease $\Delta\rho(B) = \rho(0) - \rho(B)$ is shown in Figs. 2a (paramagnet) and 2b (ferromagnet). For $T > T_C$ a full saturation of $\Delta\rho$ was not observed, even in a field of 50 T. Hysteresis effects were neither notable for the paramagnet nor for the ferromagnet due to the very small coercive fields of manganites.

Before discussing the magnetoresistive behavior it is important to note the high resistivity values (between 1 m Ω cm and 50 m Ω cm, depending on T and B as shown in Fig. 1). Relating these data to the carrier density of 0.5 holes per unit cell [9] results in a mobility between 1.4×10^{-2} cm 2 /Vs and 0.7 cm 2 /Vs. This is a very low value compared to metals, and it indicates a strong carrier localization as described by Mott's hopping model [13]. The most probable reason for this localization is the presence of local distortions of the spin lattice—like antiferromagnetic fluctuations in a ferromagnetic matrix [14]. These fluctuations cause a trapping of spin polarized carriers in a locally ferromagnetic environment, and charge transport arises from hopping and/or tunneling of carriers between these ferromagnetic entities (large spin polarons) [14]. The conductivity based on Mott hopping is given by [13,15]

$$\rho^{-1} = \sigma = e^2 R^2 \nu_{\text{ph}} N(E_F) \exp\left(-\frac{2R}{L} - \frac{W_{ij}}{k_B T}\right), \quad (1)$$

where R is the main hopping distance, ν_{ph} the phonon frequency, $N(E_F)$ the Fermi density of states, L the carrier localization length, and W_{ij} the potential energy difference (effective hopping barrier) between the hopping sites i and j . All parameters, except for L , can be either measured or estimated. The average hopping distance

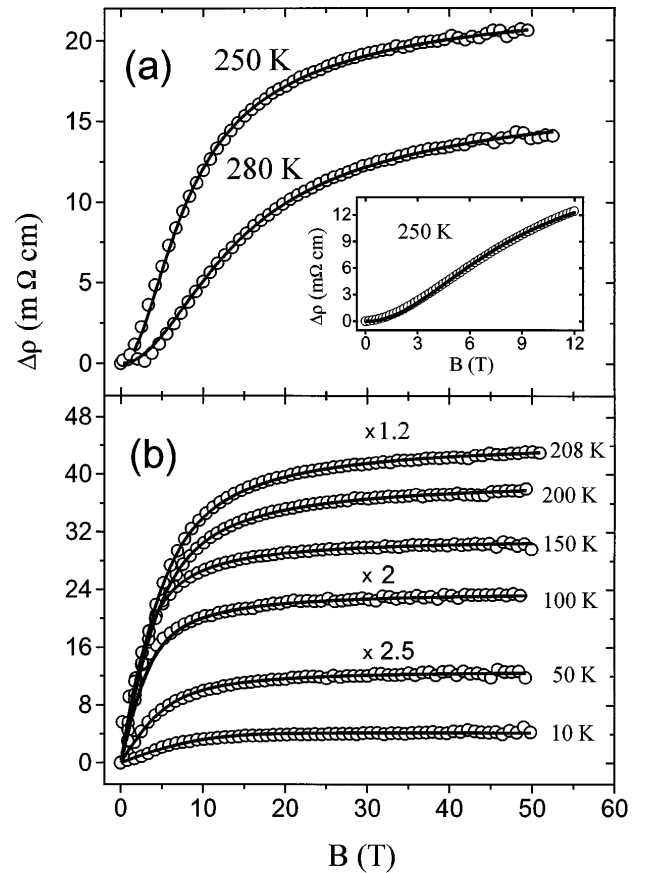


FIG. 2. The upper panel (a) shows the field dependence of the resistivity decrease in the paramagnetic phase, nicely following the square of the Brillouin function \mathcal{B} , plotted as a thin solid line. Data taken in a superconducting magnet are given in the insert of (a). The lower panel (b) shows the direct proportionality between the resistivity decrease and \mathcal{B} in the ferromagnetic regime. Curves at several temperatures are multiplied with the indicated figures to improve clarity.

corresponds to roughly 1.5 unit cells (1.5×3.82 Å), since hopping in a given direction spans over one unit cell in case the nearest-neighbor site is free (50% probability for the given substitution ratio) and over two (or more) unit cells if this site is occupied. From the Arrhenius plot of $\rho(T, B = 0)$ we deduce $W_{ij} = 55$ meV, and $\nu_{\text{ph}} \approx 2.1 \times 10^{13}$ s $^{-1}$ (estimated Raman shift of 700 cm $^{-1}$ for optical Mn-O modes). $N(E_F)$ can be approximated by a free electron model from the doping-induced carrier concentration if we assume an effective mass $m^* \approx 10m_e$, typical for strongly correlated electrons and in the range of the heat-capacity results on La manganites [14]. Using these parameters and the $\rho(0)$ data for $T > 220$ K gives a localization length $L = 10.2$ Å. This value, corresponding to 2.5 lattice constants, is physically meaningful and gives confidence in the validity of the employed model.

In the following we will apply Mott's formalism not only in the semiconducting state, but also in the quasimetallic regime. This approach gives the possibility

to deduce the temperature and field dependence of $\rho(T, B)$ in the two different magnetic phases from a common underlying mechanism. A theoretical model based on variable range hopping with barriers due to magnetic disorder was recently also published by Viret *et al.* [16]. The basic idea for this extension of Mott's model is the assumption that the hopping barrier W_{ij} can be modified by adding an extra term ΔW_{ij} . This term represents the energy related to the relative orientation of the local magnetization vectors \vec{M}_i and \vec{M}_j at both sites of a hopping process:

$$W_{ij} \longrightarrow W_{ij} - \Delta W_{ij} = W_{ij} - \alpha \vec{M}_i \cdot \vec{M}_j. \quad (2)$$

The energy barrier is therefore reduced for a ferromagnet ($\vec{M}_i \parallel \vec{M}_j$), and enhanced for a paramagnet or antiferromagnet. The proportionality constant α includes terms for consistency of dimensions and for the overlap between spin-polarized electrons and their locally magnetized environment. This picture explains qualitatively the metalliclike decrease of ρ below T_C : Increasing magnetic order favors a parallel alignment of neighboring moments, which causes in turn a lowering of W_{ij} and ρ . It is, however, not possible to estimate the evolution of W_{ij} from the $\rho(T < T_C)$ data due to the unknown temperature dependences of L and R . It might be assumed that L increases with decreasing temperature (carrier delocalization lowers the kinetic energy) while R may not vary significantly because the most probable hopping events happen on a scale of a few lattice constants. Therefore we will restrict the discussion to the magnetoresistance at fixed temperatures, allowing us to treat all quantities with unknown temperature dependence as proportionality constants. Rewriting Eq. (1) in terms of the magnetic barrier contribution ΔW_{ij} and summarizing the forefactors in ρ_0 gives

$$\frac{\Delta\rho(B, T)}{\rho_0} = \frac{\rho_0 - \rho(B)}{\rho_0} = 1 - \exp\left(-\frac{\Delta W_{ij}}{k_B T}\right) \approx \frac{\Delta W_{ij}}{k_B T}. \quad (3)$$

The absolute resistivity decrease $\Delta\rho(B, T)$ scales therefore (assuming $\Delta W_{ij} < k_B T$) like $\Delta\rho(B, T) = A(T)\vec{M}_i \cdot \vec{M}_j$. The prefactor $A(T)$ represents essentially the ratio $\rho_0/k_B T$, which depends on temperature but not on the external magnetic field. For the further evaluation of the magnetic term $\Delta W_{ij} \propto \vec{M}_i \cdot \vec{M}_j$ we take into account that the local magnetizations $\vec{M}_{i,j}$ are the sum of two different contributions: the Weiss magnetization \vec{M}_W , which is common to both sites i and j , and the local corrections $\delta\vec{M}_{i,j}$, representing the difference between M_W and the magnetically saturated state M_s , i.e., $|\delta\vec{M}_{i,j}| = |M_s - M_W|_{i,j}$. Without external magnetic field the local corrections are arbitrarily oriented, giving no effective contribution to the total magnetization. Nonzero fields induce an alignment of M_W along the field direction and cause also a common orientation of $\delta\vec{M}_{i,j}$ along this axis.

This additional contribution to the total magnetization might be approximated by the Brillouin function \mathcal{B} . The magnetic part of the barrier can thus be expressed as follows, with overlines indicating statistical averages:

$$\begin{aligned} \Delta W_{ij} &\propto \overline{(\vec{M}_W + \delta\vec{M}_i) \cdot (\vec{M}_W + \delta\vec{M}_j)} \\ &= \overline{\vec{M}_W \cdot \vec{M}_W} + \overline{\vec{M}_W \cdot (\delta\vec{M}_i + \delta\vec{M}_j)} \\ &\quad + \overline{\delta\vec{M}_i \cdot \delta\vec{M}_j}. \end{aligned} \quad (4)$$

The meaning of the three terms in Eq. (4) becomes evident within the different magnetic phases. The Weiss magnetization is absent for the paramagnet ($M_W = 0$) and Eqs. (3) and (4) predict a resistivity decrease $\Delta\rho(B, T) = A(T)\delta\vec{M}_i \cdot \delta\vec{M}_j$. $A(T)$ plays hereby the role of a temperature-dependent CMR amplitude. The average component of $\delta\vec{M}_{i,j}$ along the field direction is supposed to scale with the Brillouin function \mathcal{B} , and the total resistivity decrease scales therefore with $\mathcal{B}^2(g\mu_B J(T)B/k_B T)$, where $g = 2$ is the gyromagnetic ratio, μ_B the Bohr magneton, and $J(T)$ the average spin moment at the hopping sites. Figure 2a shows the excellent agreement between the fit function $A(T)\mathcal{B}^2$ and the $\Delta\rho(B)$ data in the paramagnetic regime up to 50 T. Especially the crossover from the parabolic CMR effect in small fields to negative curvature and saturation in high fields is correctly reproduced. A measurement in a superconducting magnet shows the validity of the \mathcal{B}^2 scaling with improved low-field resolution (inset of Fig. 2a).

In the ferromagnetic state ($M_W \neq 0$) the absolute value of the correction terms $\delta\vec{M}_{i,j}$ is small compared to the Weiss magnetization. The decrease of the energy barrier is therefore dominated by the first two terms in Eq. (4), and the third term can be ignored. Already without external field the resistivity decreases with decreasing temperature due to the increasing Weiss field; compare also Fig. 1. The additional CMR effect should be proportional to the second term of Eq. (4), i.e., $\Delta\rho(B, T) = A(T)\mathcal{B}[g\mu_B J(T)B/k_B T]$, assuming again that the component of the correction terms follows the Brillouin scaling. The solid lines in Fig. 2b show the applicability of this Brillouin fit in the ferromagnetic regime up to T_C .

The temperature dependence of the spin moment J and the amplitude parameter A is given in Fig. 3. The very high moments ($J \approx 60$ at 200 K, whereas $J = 2$ for a bare Mn^{3+} ion) indicate that the Nd perovskite behaves as a superparamagnet under formation of magnetically aligned clusters with an extension of typically three lattice constants. These clusters might be interpreted in terms of the "large spin polarons" introduced in Ref. [14]. Moreover, this cluster size agrees well with the carrier localization length calculated above from Eq. (1) (10.2 Å) and with the magnetic-polaron diameter (12 Å) determined by De Teresa *et al.* [5]. The data in Fig. 3 suggest a slight increase of the cluster size by approaching T_C from

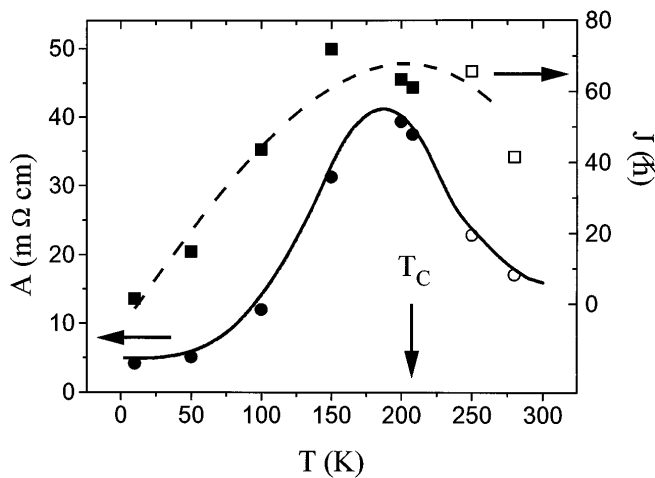


FIG. 3. Temperature dependence of the fit parameters $A(T)$ and spin moment $J(T)$. The solid dots refer to the simple \mathcal{B} fit, open dots to the \mathcal{B}^2 fit. The temperature dependence of $A(T)$ follows the $\rho_0(T)$ behavior (solid line) and the absolute values of $J(T)$ indicate a superparamagnetic behavior. The dashed line through the $J(T)$ data is a guide to the eye.

temperatures above. Below T_C we suppose $J(T)$ to decrease gradually to zero, because $|\delta M_{i,j}| = M_s - M_W = 0$ for $T \rightarrow 0$, which is consistent with the experimental result. In this scenario the carriers are mobile and delocalized within the individual clusters, while the macroscopic resistivity is determined by the magnetically impeded transfer of carriers between adjacent spin clusters.

The amplitude A follows closely the temperature variation of ρ_0 , and the residual resistivity in the limit of magnetic saturation $\rho_s(T) = \rho_0(T) - A(T) = 0.7 \pm 0.2$ m Ω cm is almost temperature independent. This constant ρ_s value, according to Eq. (1), implies a $W_{ij} = 0$, compare also Ref. [16]. Using Eq.(1) and a cluster diameter of 12 Å as localization length results in $\rho_s = 2.7$ m Ω cm, slightly higher than the above value. This difference might arise from a variation of the parameters L and R under the very high external fields.

In summary, we have applied Mott's hopping model to a colossal magnetoresistive material by introducing a barrier contribution depending on the relative spin orientation at the hopping sites. This approach deduces the semiconducting and the quasimetallic transport properties from a universal mechanism, which determines the temperature coefficient and the absolute value of resistivity via the magnetization-controlled hopping barrier. Ex-

pressing the average mutual spin orientation in terms of the external magnetic field produces a remarkable simple CMR dependence proportional to the Brillouin function in the ferromagnetic phase. The paramagnetic state without prominent magnetization axis is characterized by a CMR effect following a squared Brillouin function. Both relations hold over a very broad field range up to 50 T. The residual resistivity at magnetic saturation is nearly temperature independent, and its value indicates a semiconducting or itinerant metallic transport mechanism.

This work was supported by the Flemish Concerted Action, the Fund for Scientific Research-Flanders, and the Belgian Interuniversity Attraction Poles programs. P.W. acknowledges financial support by the TMR program of the European Union. The authors thank M.J. Van Bael and A. Vantomme for magnetization and RBS measurements.

*Corresponding author: Laboratorium voor Vaste-Stoffysica en Magnetisme, Katholieke Universiteit Leuven, Celestijnenlaan 200 D, 3001 Leuven, Belgium. Electronic address: Patrick.Wagner@fys.kuleuven.ac.be

- [1] R.M. Kusters *et al.*, *Physica* (Amsterdam) **155B**, 362 (1989); R. von Helmolt *et al.*, *Phys. Rev. Lett.* **71**, 2331 (1993).
- [2] For a review see A.P. Ramirez, *J. Phys. Condens. Matter* **9**, 8171 (1997).
- [3] P.G. Radaelli *et al.*, *Phys. Rev. Lett.* **75**, 4488 (1995).
- [4] H. Kawano *et al.*, *Phys. Rev. Lett.* **78**, 4253 (1997).
- [5] J.M. De Teresa *et al.*, *Nature* (London) **386**, 256 (1997).
- [6] P.G. de Gennes, *Phys. Rev.* **118**, 141 (1960), and references therein.
- [7] A.J. Millis *et al.*, *Phys. Rev. Lett.* **74**, 5144 (1995).
- [8] Guo-meng Zhao *et al.*, *Nature* (London) **381**, 676 (1996).
- [9] P. Wagner *et al.*, *Europhys. Lett.* **41**, 49 (1998).
- [10] M.F. Hundley *et al.*, *Appl. Phys. Lett.* **67**, 860 (1995); J. O'Donnell *et al.*, *Phys. Rev. B* **54**, R6841 (1996); B. Martínez *et al.*, *ibid.* **54**, 10001 (1996).
- [11] P. Wagner *et al.*, *Phys. Rev. B* **55**, 3699 (1997).
- [12] F. Herlach *et al.*, *Physica* (Amsterdam) **216B**, 161 (1996).
- [13] N.F. Mott and E.A. Davis, *Electronic Processes in Non-Crystalline Materials* (Clarendon Press, Oxford, 1979).
- [14] J.M.D. Coey *et al.*, *Phys. Rev. Lett.* **75**, 3910 (1995).
- [15] The limited semiconductor regime in Fig. 1 does not allow for a distinction between nearest-neighbor, Shklovskii-Efros, variable-range, and polaron hopping. Employing Mott's model is justified provided that a quantum coherent state is stable in the whole temperature regime.
- [16] M. Viret *et al.*, *Phys. Rev. B* **55**, 8067 (1997).